Optical Materials 137 (2023) 113533

Contents lists available at ScienceDirect

Optical Materials

journal homepage: www.elsevier.com/locate/optmat

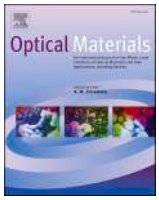

Research Article

# Down-shifting photoluminescent properties of $Tb^{3+}$ doped phosphate glasses for intense green-emitting devices applications

Kartika Maheshwari [a,b], A.S. Rao [a,*]

[a] Department of Applied Physics, Delhi Technological University, Bawana Road, Delhi, 110042, India
[b] ABES Engineering College, Ghaziabad, Uttar Pradesh (U. P.), 201 009, India

ARTICLE INFO

*Keywords:*
Phosphate glass
Optical bandgap
PL properties
PL Decay
Thermal stability

ABSTRACT

$Tb^{3+}$ doped BZLP glasses were prepared via a melt-quenching route and investigated thoroughly using spectroscopic techniques such as XRD, UV-VIS absorption and photoluminescence (PL) to explore their utility in visible photonic device applications. The information pertaining to glass transition temperature, melting temperature, and thermal stability were understood by using recording the differential scanning calorimetry (DSC) spectrum for an undoped BZLP glass. The total weight loss during the glass composition melting process was analyzed using Thermogravimetric curves. The UV spectral information recorded for the titled glasses reveals the optical bandgap falling in the range from 4.57 to 4.19 eV. The prepared $Tb^{3+}$ doped BZLP glasses exhibit intense green emission along with relatively less intense blue, yellow, and red peaks under 373 nm excitation. In the resultant PL spectra, the emission intensity increases with the activator concentration of $Tb^{3+}$ ions from 0.5 to 5.0 mol%. The estimated CIE chromaticity coordinates falling in the green region reveal the aptness of the titled glasses as a green constituent in visible photonic devices. The PL decay curves show the bi-exponential behavior with an average decay time of 2–3 ms. The temperature-dependent PL profile shows fewer changes in spectra and has a relatively high activation energy value, confirming the high thermal stability. Various results obtained for $Tb^{3+}$ doped BZLP glasses finally reveal their usage as a green emitter needed to fabricate w-LEDs and other green-emitting photonic device applications.

## 1. Introduction

Over the last few decades, the fabrication of rare-earth (RE) activated inorganic glasses have received a lot of attention because of their significant role in the advancement of photonic devices and their applications [1–4]. Furthermore, RE doped glasses have specific properties such as high luminous efficiency, thermal resistance, chemical stability, extended durability, low production cost, and many more, which can position them as a critical player in the field of science and technology [4,5]. These different properties of RE doped glasses are required in many sectors and multiple advantageous applications to build sophisticated display devices, variable power lasers, solar cells, optical fibers, waveguides, optical memory systems, advanced lighting devices, sensors, and so on [6–9]. Modern lighting devices, such as white light emitting diodes (w-LEDs), are replacing traditional and long-lasting illuminating systems. The RE doped glasses are one of the utmost promising materials for fabricating w-LEDs since they can overcome the disadvantages of phosphor materials, do not require organic epoxy resins, and have no aging effects [10]. Furthermore, the RE activated glasses act as an appropriate wavelength converters as well as an encapsulant in the fabrication of w-LEDs [11].

The luminescent features of the RE doped glasses depend not only on the RE ions but also on the host matrix that provides a crystal field environment to the RE ions. As a result, selecting a glass host matrix is equally important along with the choice of a particular RE ion for the designated applications. Out of many host glass matrices, the phosphate glass host offers outstanding features such as high thermal stability, reduced melting point, thermal resistance, chemical durability, high transparency and many more. These unique properties of phosphate glasses motivated us to explore more about them [6,12–14]. An alkaline oxide, such as BaO, can be used as a network modifier in phosphate glass formers, forming non-bridging oxygen groups and lowering the melting temperature of the glass host [15,16]. Adding alkali oxides helps to minimize the non-radiative losses that lead to the enhancement of the luminescence characteristics. Furthermore, alkali oxides such as lithium oxide added to a phosphate glass increas the transition temperature. The

* Corresponding author.
*E-mail address:* drsrallam@gmail.com (A.S. Rao).

https://doi.org/10.1016/j.optmat.2023.113533
Received 7 December 2022; Received in revised form 13 January 2023; Accepted 27 January 2023
Available online 7 February 2023

only setback with phosphate glasses is their hygroscopic nature which can be mitigated considerably by adding zinc oxide to it. The addition of ZnO can modify P–O–P to P–O–Zn bonds and improves moisture-resistant characteristics [17,18]. All the aforementioned special characteristic features owned by the constituent chemical substances such as BaO, ZnO, $Li_2O$ and $P_2O_5$ motivated us to synthesize barium zinc lithium phosphate (BZLP) glass system doped with distinct RE ions to understand the suitability of the BZLP host glass for numerous photonic device applications.

The desired luminescence characteristics of Lanthanide ions in tri/divalent states show the different energy states in UV to the IR region of the electromagnetic spectrum, making available a broad range and producing visible lasers and other photonic device applications. In lanthanides ions, mostly a sharp excitation and sharp radiative emission ($f-f$ transitions) were perceived due to the partially filled 4*f* shells shielded by $5s^2 5p^6$ orbitals [19]. The highest effective green emitting PL ingredient among the RE ions was found when the host was activated with $Tb^{3+}$ ions. The PL properties of $Tb^{3+}$ ions in the host were determined by $^5D_4 \rightarrow {}^7F_j$ transitions, which were affected by the amount of $Tb^{3+}$ ions doped, the composition of the surrounding host, and the pumping wavelength [18,19]. Long lifetime, high quantum efficiency, and narrow emission spectral width can make $Tb^{3+}$ ions contained molecules more suitable for many distinctive applications such as biological probes, green color components in displays, sensors, thermos luminescent dosimeters, field emission displays, and other photonic devices [20–22]. Many researchers have recently investigated $Tb^{3+}$ doped glasses for luminous device applications.

Due to the distinctive optical characteristics and direct applicability of RE induced glassy systems in diversified areas, $Tb^{3+}$ doped BZLP glasses have been prepared and studied for its spectroscopic properties. UV–vis absorption, luminescence properties, and lifetime profiles were used to distinguish the suitability of the $Tb^{3+}$ incorporated BZLP glass for appropriate w-LEDs and luminescent devices applications.

## 2. Experimental section

### 2.1. Synthesis

$Tb^{3+}$ ion doped BZLP glass samples have been synthesized using melt quenching process with molar composition given below:

$60P_2O_5$ –15ZnO-(15-*m*) BaO -$10Li_2O$: *m*$Tb_4O_7$where *m* = 0.5, 1.0, 1.5, 2.0, 2.5, 3.0, 3.5, 4.0, 4.5 and 5.0 mol% in BZLP glasses abbreviated as $PZBaLTb_{0.5}$, $PZBaLTb_{1.0}$, $PZBaLTb_{1.5}$, $PZBaLTb_{2.0}$, $PZBaLTb_{2.5}$, $PZBaLTb_{3.0}$, $PZBaLTb_{3.5}$, $PZBaLTb_{4.0}$, $PZBaLTb_{4.5}$ and $PZBaLTb_{5.0}$ respectively. Here *m* signifies the doping content of $Tb^{3+}$ ions. Fig. 1 indicates the steps followed to prepare the aforementioned glasses through the most commonly used melt quenching technique. The transparent and uniformed glasses were obtained and ready for further characterization at ambient temperature.

### 2.2. Characterization

The density of the as-prepared glasses has been calculated using Archimedes' principle in the distilled water medium. DSC-TGA data were recorded in the range of 50–1300 °C by DSC/TGA real-time instrument (SETARAM, Labsys Evo). The XRD has been recorded to confirm the glassy nature of the titled glasses (D8 advance, Bruker). The absorption spectral studies have been done via spectrophotometer (JASCO, V-770). Photoluminescence excitation and emission spectra were recorded via Spectro fluorophotometer (JASCO, 8300 FP) at 300 K. The lifetime measurements were investigated via spectrophotometer (Horiba, Fluorolog-3). The temperature-dependent PL (TD-PL) studies have been performed using a spectrophotometer (FLAME- S-XR1-ES, Ocean optics) with a heating sample assembly.

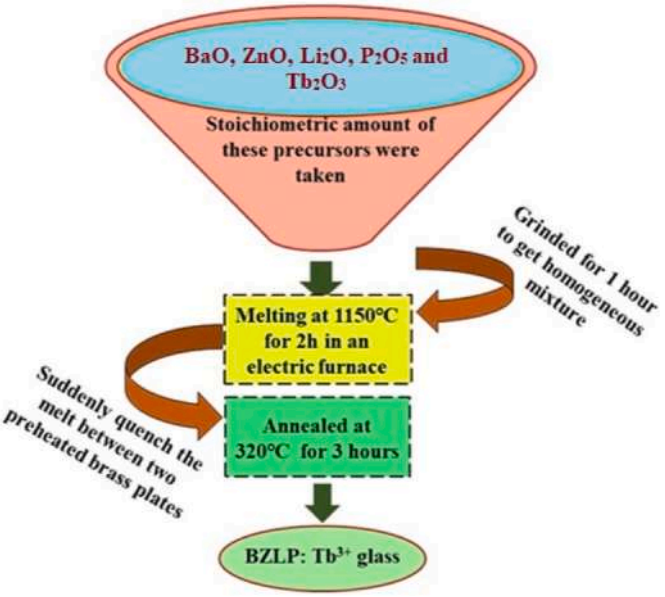


**Fig. 1.** Schematic diagram of a melt-quenching technique.

## 3. Results and discussion

### 3.1. DSC/TGA analysis

The DSC curve for the undoped BZLP glass has been plotted in the range of 50–1300 °C, as presented in Fig. 2. It contains various endo as well as exothermic peaks. The values of glass melting, peak crystallization, onset crystallization, and transition temperature were found to be $T_m$ = 1193 °C, $T_p$ = 226 °C, $T_c$ = 179 °C, and $T_g$ = 157 °C, respectively. The thermal stability of the as-prepared glass composition can be analyzed on the basis of temperature difference (ΔT) and thermal stability parameter (S). These two critical parameters can be estimated by using the following expressions [11,20].

$$\Delta T = T_p - T_g \tag{1}$$

$$S = \frac{(T_p - T_c)(T_c - T_g)}{T_g} \tag{2}$$

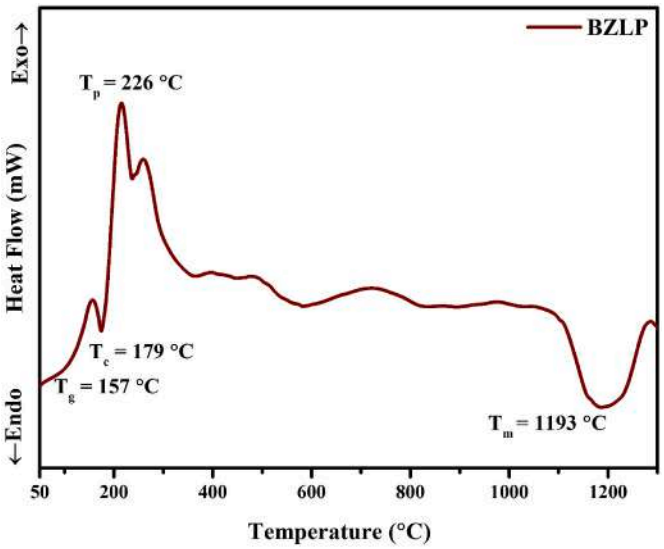


**Fig. 2.** DSC curve for an undoped BZLP glass.

The ΔT value signifies the range of temperature where the material can endure crystallization through any type of heat treatment. Here it was found to be 69 °C which is relatively higher than the other reported values [21]. Such a significant value reveals that the as-prepared glass is thermally stable. Furthermore, the value of S was found to be 6.58. Also, the endothermic peak observed at 1193 °C indicates the melting temperature of the glass composition, which is used for glass preparation. Based on the observed values of ΔT and S, the undoped BZLP glass may be considered a good host for photonic device applications.

Fig. 3 shows the two stages of weight loss in the TGA curve plotted for an undoped BZLP host glass. The first weight loss was observed between 50 and 600 °C and the corresponding loss was found to be 21.38%, owing to water molecules and ammonia. It means the reaction happening is an exothermic reaction. This is in correlation with the outcomes of the DSC curve. The second stage of the weight loss at 600 °C ascribed because of the release and decomposition of $CO_2$ gas, which was found to be 10.47%. Initially, we have taken a sample amount is 35.67 mg, which is homogeneously mixed. After heating it to 1300 °C, the remaining sample is 24.26 mg. Hence, a total of 68.15% of the weight remained after the preparation of BZLP glass.

### 3.2. Physical properties

The density of $Tb^{3+}$ doped BZLP glasses was determined based on the experimental approach. Several physical parameters were estimated including average molecular weight, molar reflection and refraction losses (R), dielectric constant ($\varepsilon$), electronic polarizability (e), and optical electronegativity ($\chi_{opt}$) by following the expressions from already published papers [22].

The increase in $Tb^{3+}$ ions concentration increases the value of the refractive index (n) and density (d) in BZLP glasses. A heavy weight of $Tb_4O_7$ is responsible for an increase in the molecular weight of the glass samples, which could explain the increase in density. By linking the oxygen atom to $Tb^{3+}$ ions in BZLP glasses, the incorporation of $Li_2O$ in our host matrix produces non-bridging oxygen and helps to improve the network stability. In addition, the inter-ionic radius ($r_i$) and the polaron radius ($r_p$) of the as-synthesized BZLP glasses decrease with the $Tb^{3+}$ ion content. All these physical parameters have been depicted in Table 1.

The increase in field strength (F) signifies that the bond strength between Tb and O is increasing, and tri-borate units are converting into tetra-borate units [23]. With an increase in $Tb^{3+}$ ions concentration, some more parameters such $\varepsilon$ and R are also increasing. The variation in all these physical parameters tells the behaviour of the as-prepared glass with change in concentration of RE ions.

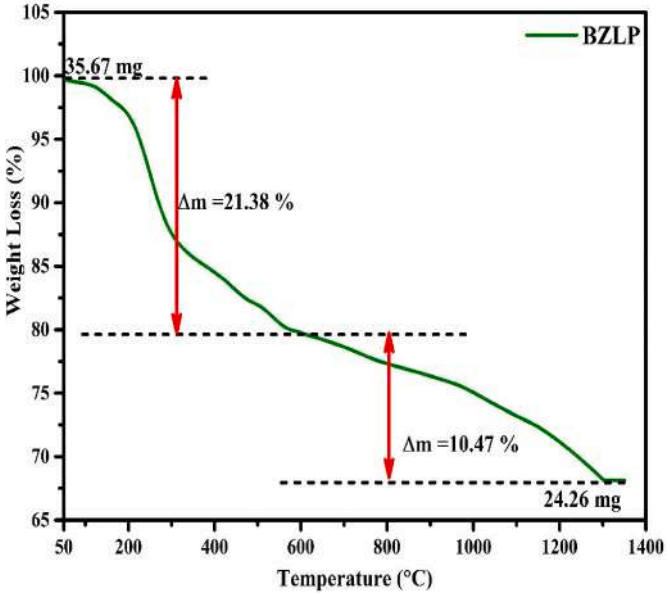


**Fig. 3.** TGA curve for an undoped BZLP glass.

### 3.3. Structural analysis

XRD was performed to confirm the glassy nature of the titled glasses. The XRD patterns investigated for all (undoped as well as doped) glasses are the same, so we have shown the XRD pattern of $PZBaLTb_{5.0}$ glass only in Fig. 4. It has only a large hump about an angle of 28 °C without any solid crystalline peak, which discloses the non-crystalline and glassy characteristics of the as-prepared glasses.

### 3.4. Absorption properties of glass

Fig. 5 illustrates the absorption spectra recorded for $Tb^{3+}$ doped BZLP glasses in the range of 250–500 nm. It consists eight peaks at 284, 302, 318, 339, 350, 370, 379 and 484 nm related to f-f- transitions of $Tb^{3+}$ ions based on the Carnall report [24]. The electric dipole-induced transitions followed the selection rule $|J| \leq 6$, whereas the magnetic dipole-induced transition followed $|J| = 0,+1$.

Using the absorption spectra, the optical band gap of $Tb^{3+}$ doped glasses was estimated by employing the Davis and Mott relation as follows [12]:

$$\alpha(\nu) = \left(\frac{B}{h\nu}\right)\left(h\nu - E_{opt}\right)^n \quad (3)$$

here, $h\nu$ is photon energy, $E_{opt}$ is the optical bandgap of glass, and B is the band tailing parameter. The parameter n is a number that declares the type of transition. The value $n = 1/2$ denotes the indirect allowed transitions. The $\alpha(\nu)$ was estimated by using the expression [25]:

$$\alpha(\nu) = \left(\frac{1}{d}\right) ln\left(\frac{I_0}{I_T}\right) \quad (4)$$

Here $d$ is glass thickness and the absorbance represents by the factor $ln(I_0/I_T)$. The $E_{opt}$ values for $Tb^{3+}$ doped glasses were evaluated for indirectly allowed transitions via Tauc plot, as presented in Fig. 6. These values were found in the range of 4.57–4.19 eV and placed in Table 1.

### 3.5. PL analysis

PL excitation spectra of the as-prepared glasses were recorded in 250–500 nm range by fixing emission wavelength at 545 nm. The excitation spectrum in Fig. 7, exhibits many excitation peaks. The excitation peaks were detected at 284, 302, 318, 339, 350, 368, 375, and 485 pertaining the transitions from ground level ($^7F_6$) to various energy levels $^5F_4$, $^5H_6$, $^5H_7 + {}^5D_0$, $^5L_7 + {}^5G_3$, $^5L_9 + {}^5D_2$, $^5G_5$, $^5G_6 + {}^5D_3$, and $^5D_4$ of $Tb^{3+}$ ions, respectively [26,27]. The dominant excitation peak was observed at 373 nm corresponding to the transition from the lowest energy state $^7F_6$ ($4f^8$) to the higher spin–allowed excited state $^5H_6$ ($4f^7 5d^1$) of the $Tb^{3+}$ ion. Hence, the as-prepared glasses have been effectively excited by that n-UV excitation source. Further, this excitation wavelength (373 nm) was chosen to record the PL emission spectra of $Tb^{3+}$ doped BZLP glasses.

The PL spectra of BZLP glasses doped with the varying concentration of $Tb^{3+}$ ions under 373 nm excitation wavelength shown in Fig. 8. The resulting PL profile exhibits several peaks in the range of 450–700 nm. The blue, green, yellow and red emission peaks were situated at 490, 542, 585 and 620 nm due to the characteristic transitions $^5D_4 \rightarrow {}^7F_6$, $^7F_5$ $^7F_4$ and $^7F_3$ of $Tb^{3+}$ ions, respectively. The blue emission peak related to the $^5D_4 \rightarrow {}^7F_6$ transition followed the selection rule $\Delta J = \pm 1$ rule and magnetic dipole in nature. The green emission peak arises due to the $^5D_4 \rightarrow {}^7F_5$ transition following the Laporte-forbidden selection rule, which is the most intense among all the emission peaks [14,28–30]. In the resultant PL spectra, the emission intensity changed with a surge in the

**Table 1**
Physical parameters of $Tb^{3+}$ doped BZLP glasses.

| Physical Property | PZBaL $Tb_{0.5}$ | PZBaL$Tb_{1.0}$ | PZBaL $Tb_{2.0}$ | PZBaL $Tb_{3.0}$ | PZBaL $Tb_{4.0}$ | PZBaL $Tb_{5.0}$ |
|---|---|---|---|---|---|---|
| Refractive index ($n_d$) | 2.06 | 2.12 | 2.13 | 2.13 | 2.14 | 2.14 |
| Density (gm/$cm^3$) | 3.02 | 3.04 | 3.20 | 3.21 | 3.26 | 3.33 |
| Average molecular weight | 211.51 | 214.47 | 220.41 | 226.35 | 232.30 | 238.24 |
| $Tb^{3+}$ion concentration N ($10^{22}$ ions/$cm^3$) | 0.4278 | 0.8691 | 1.7254 | 2.5424 | 3.3276 | 4.0823 |
| Polaron radius ($r_p$) (Å) | 2.4836 | 1.9602 | 1.5467 | 1.3703 | 1.2453 | 1.1705 |
| Inter-atomic distance ($r_i$) (Å) | 61.6329 | 48.6232 | 38.736 | 34.0098 | 31.1092 | 29.0502 |
| Optical band gap (eV) | 4.57 | 4.38 | 4.32 | 4.27 | 4.21 | 4.19 |
| Dielectric constant (Ɛ) | 4.2759 | 4.4106 | 4.4549 | 4.4926 | 4.5387 | 4.5538 |
| Optical dielectric constant (Ɛ-1) | 3.2759 | 3.4106 | 3.4549 | 3.4926 | 3.5387 | 3.5538 |
| Molar refraction ($R_m$) ($cm^{-3}$) | 18.493 | 19.098 | 19.382 | 19.656 | 19.723 | 19.784 |
| Reflection losses (R %) | 6.883 | 7.418 | 7.487 | 7.522 | 7.582 | 7.698 |

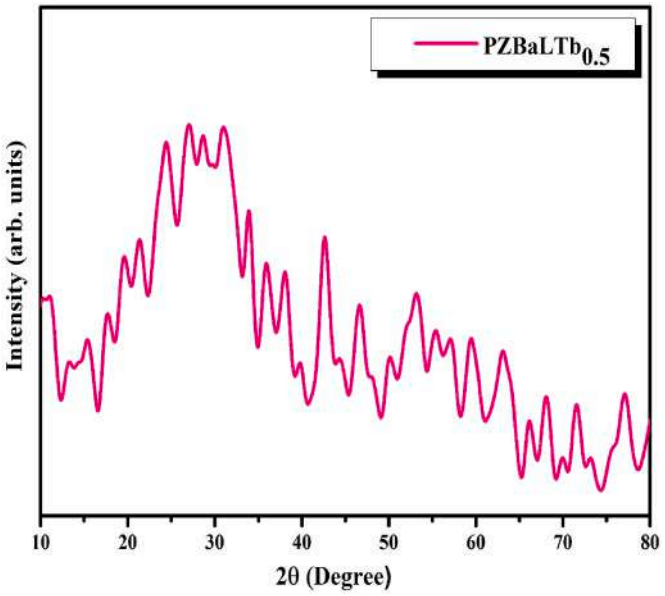


**Fig. 4.** XRD pattern of 5.0 mol% $Tb^{3+}$ doped BZLP glass ($PZBaLTb_{5.0}$).

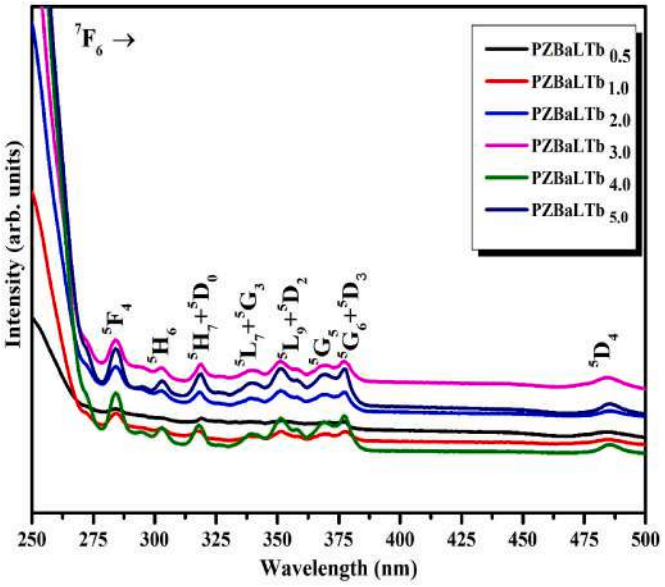


**Fig. 5.** Absorption spectra of $Tb^{3+}$ doped BZLP glass with variable concentration of $Tb^{3+}$ ions.

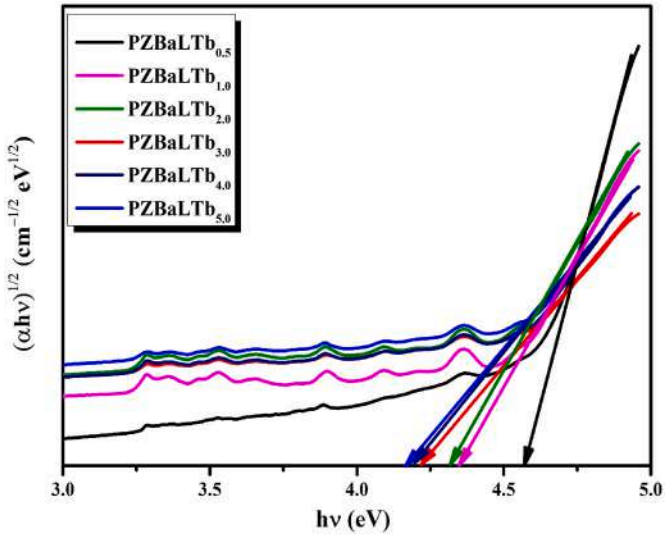


**Fig. 6.** Tauc plot of $Tb^{3+}$ doped BZLP glasses.

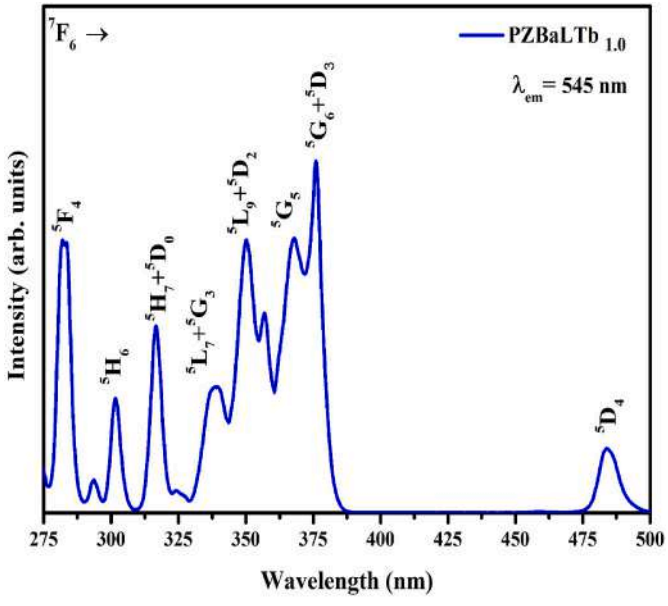


**Fig. 7.** The excitation spectrum of the $PZBaLTb_{1.0}$ glass with monitoring the emission wavelength at 545 nm.

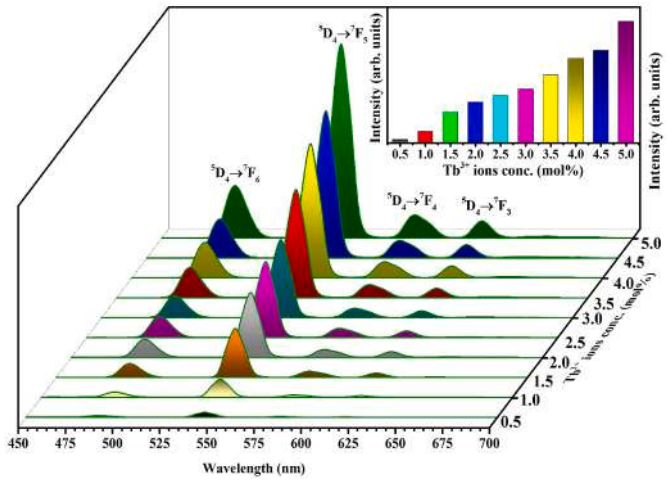


**Fig. 8.** PL spectra of $Tb^{3+}$ doped BZLP glasses with the doping concertation varying from 0.5 to 5.0 mol% at 373 nm excitation wavelength. The inset plot shows the variation of the emission intensity with $Tb^{3+}$ ions concentration.

doping concentration of $Tb^{3+}$ ions in BZLP glasses. The emission intensity intensifies with an increase in activator concentration of $Tb^{3+}$ ions from 0.5 to 5.0 mol%. No concentration quenching was observed up to 5.0 mol% of $Tb^{3+}$ ions in BZLP glasses. This is another key feature of the BZLP glass host having high RE solubility and can be suitable for photonic applications. The ratio between blue ($^5D_4 \rightarrow {}^7F_6$) and green ($^5D_4 \rightarrow {}^7F_5$) emission peaks defines the center of symmetry around the $Tb^{3+}$ ions in BZLP glasses. Hence the green color (G) to blue color (B) ratio was evaluated, which was reckoned to be more than four and varies with activator ions content. The high value of the G/B ratio recommends no center of symmetry around the $Tb^{3+}$ ions in BZLP glasses [29].

Fig. 9 illustrated the partial energy level of $Tb^{3+}$ doped BZLP glasses, which clarified the excitation, radiative and non-radiative transitions mechanism involved. It is represented that $Tb^{3+}$ ions were excited at 373 nm wavelength and populated the energy level. The occupied $^5D_3$ excited energy level may release the energy in two ways, initially some non-radiative relaxation up to the $^5D_4$ level. Finally, radiative emission occurs from the $^5D_4$ to $^7F_{6\text{-}3}$ levels of $Tb^{3+}$ ions in BZLP glasses, giving

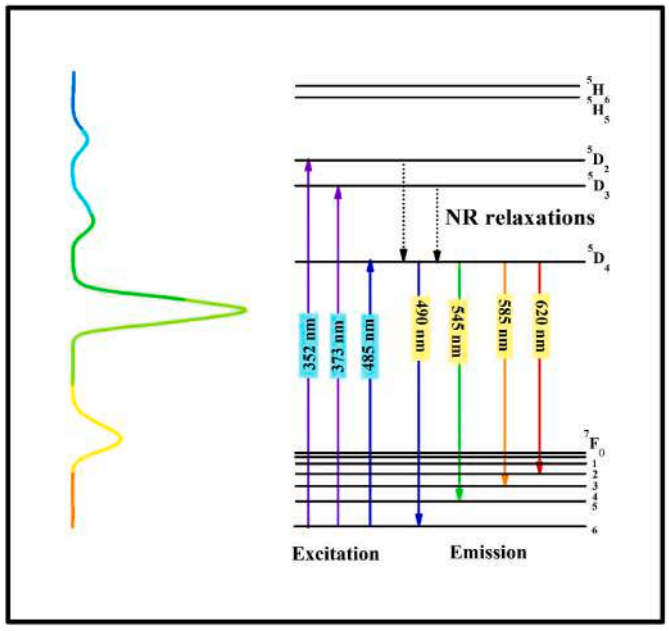


**Fig. 9.** Partial energy level diagram of $Tb^{3+}$ doped BZLP glasses.

visible blue, green, yellow and red light in the range of 450–700 nm [31].

### 3.6. Colorimetric study

The recorded emission profiles under 373 nm excitation for $Tb^{3+}$ doped BZLP glasses were used to evaluate chromaticity color coordinates. The chromaticity coordinates for all glasses were tabulated in Table 2. All the evaluated coordinates were situated in the green region of the CIE diagram. The chromaticity coordinates for $PZBaLTb_{5.0}$ glass (0.309, 0.597) as shown in Fig. 10, closely match the green emitting component by the European Broadcasting Union illuminant (0.290, 0.600). The CCT was evaluated with the help of the McCamy formula [32]:

$$CCT = -449n^3 + 3525n^2 - 6823.2n + 5520.3 \quad (5)$$

In the above relation, $n = \frac{x-x_e}{y-y_e}$, $x_e = 0.332$, $y_e = 0.186$. The emitted light can be considered as a cool green light because CCT values are greater than 5000K as placed in Table 2. Based on chromaticity coordinates, the color purity has been evaluated for all glasses by using the following expression [33–35]:

$$Color\ Purity = \sqrt{\frac{(x-x_{ee})^2 + (y-y_{ee})^2}{(x_d-x_{ee})^2 + (y_d-y_{ee})^2}} \quad (6)$$

here, $(x, y)$, $(x_d, y_d)$ and $(x_{ee}, y_{ee})$ specify the CIE coordinates of glass, dominate wavelength point and standard white point, respectively. The calculated color purity for prepared glasses is listed in Table 2. The color purity for $PZBaLTb_{5.0}$ glass was found to be 79%. The result described above favors that $Tb^{3+}$ doped BZLP glasses are very effective green emitting constituents for developing w-LEDs and other photonic devices.

### 3.7. Decay profile analysis

PL decay curves of $Tb^{3+}$ doped BLZP glasses were recorded from the $^5D_4$ level via monitoring the emission of 542 nm at 373 nm excitation, as illustrated in Fig. 11. The recorded PL decay curves at room temperature for all the glasses show the exponential behaviour. The decay curves of the as-prepared glasses were found to best fit with the bi-exponential equations as follows [28,36].

$$I = I_0 + A_1\ exp(-t/\ \tau_1) + A_2\ exp(-t/\tau_2) \quad (7)$$

Here, $I_0$ and $I$ signifies the PL decay intensities at starting (t = 0) and t time, $A_1$ and $A_2$ are the decay fitting constants, $\tau_1$ and $\tau_2$ were lifetime components. The average decay time can be estimated as per the following expression:

$$\tau_{avg} = \frac{A_1\tau_1^2 + A_2\tau_2^2}{A_1\tau_1 + A_2\tau_1} \quad (8)$$

The average decay time for the series of $Tb^{3+}$ doped glasses was listed in Table 2, which shows the minor disparity with changes in doping concertation. The average lifetime value for the $PZBaLTb_{0.5}$ glass

**Table 2**
CIE coordinates $(x, y)$, CCT (K), color purity (%) and lifetime (ms) of $Tb^{3+}$ doped BZLP glasses.

| Glass | Chromaticity coordinates | | CCT (K) | Color Purity (%) | Lifetime (ms) |
|---|---|---|---|---|---|
| | x | y | | | |
| **$PZBaLTb_{0.5}$** | 0.302 | 0.499 | 6201 | 69% | 2.893 |
| **$PZBaLTb_{1.0}$** | 0.308 | 0.562 | 5972 | 71% | 2.851 |
| **$PZBaLTb_{2.0}$** | 0.307 | 0.576 | 5971 | 73% | 2.828 |
| **$PZBaLTb_{3.0}$** | 0.307 | 0.586 | 5949 | 74% | 2.793 |
| **$PZBaLTb_{4.0}$** | 0.310 | 0.593 | 5902 | 77% | 2.757 |
| **$PZBaLTb_{5.0}$** | 0.309 | 0.597 | 5917 | 79% | 2.724 |

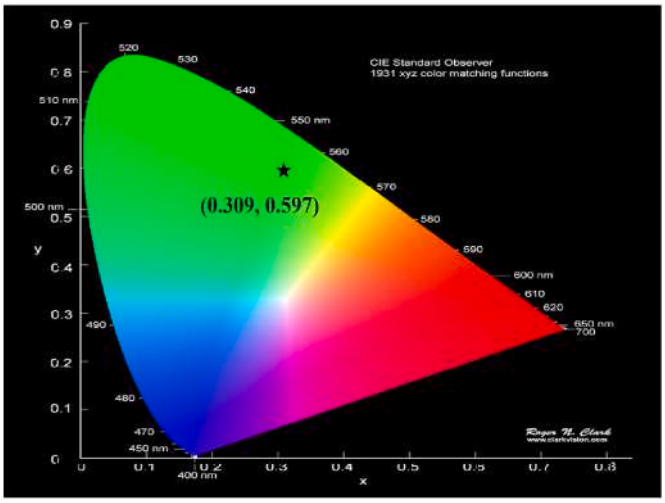


**Fig. 10.** CIE chromaticity coordinates of $PZBaLTb_{5.0}$ glass.

is 2.893 ms, which was reduced to 2.724 ms for the $PZBaLTb_{5.0}$ glass.

### 3.8. Temperature-dependent PL characteristics

To investigate the luminescence features and thermal stability of the as-prepared glasses, the TDPL spectra were recorded at different temperatures under 373 nm excitation. TDPL spectra of $PZBaLTb_{5.0}$ glass are shown in Fig. 12. The TDPL spectra reveal a slightly falling intensity with temperature rise. It may be described as thermal energy increasing with temperature. It supported the electrons to pass the point of ground and excited level, emitting energy through the non-radiative transition process. The thermal stability can be considered a direct measure of activation energy. Arrhenius equation was used to calculate the activation energy as follows [10]:

$$I_T = \frac{I_o}{1 + C\exp\left(-\frac{\Delta E}{K_B T}\right)} \tag{9}$$

where, $I_o$ and $I_T$ represent the PL intensity at room temperature (300 K) and $T\,(K)$. $\Delta E$ stands for activation energy and $K_B$ denotes the Boltzmann's constant whereas C is a random constant . The graph between $ln[(I_o/I_T) - 1]$ and $(1/K_B T)$ was plotted and fitted with a linear equation as shown in Fig. 13. Using the plotted graphs, the estimated activation energy is 0.161 eV. This high value of $\Delta E$ value proposes the high thermal stability of the present glass system, which supports the utility of the as-prepared glasses.

## 4. Conclusions

In this work, the $Tb^{3+}$ doped BZLP glasses have been synthesized using the melt-quenching technique. We have characterized the titled glasses through several techniques, analyzed and then summarized them as follows:

- The XRD pattern recorded for $Tb^{3+}$ doped glasses confirmed their glassy nature.
- UV–vis spectra were employed to estimate the energy band gap for $Tb^{3+}$ doped BZLP glasses via Tauc's plot, which is found in the range of 4.57-4.19 eV.
- The dominant emission attributed to the $^5D_4 \rightarrow {}^7F_5$ transition gave the intense green emission at 542 nm under 373 nm excitation wavelength.
- All the evaluated coordinates were situated in the green region of the CIE diagram. The chromaticity coordinates for $PZBaLTb_{5.0}$ glass (0.309, 0.597) matched with green emitting standard data.
- The PL decay profiles of $Tb^{3+}$ doped BZLP glasses are found bi-exponential in nature.
- A significantly slighter decrease in emission intensity with rising temperature and the high activation energy value (0.161 eV) suggests that the prepared glasses have good thermal stability.

The above mentioned characteristics indicate the suitability of $Tb^{3+}$ doped BZLP glasses for green color emitting components useful in various photonic device applications such as display devices and w-LEDs.

### CRediT authorship contribution statement

**Kartika Maheshwari:** work plan, experiments, calculation and

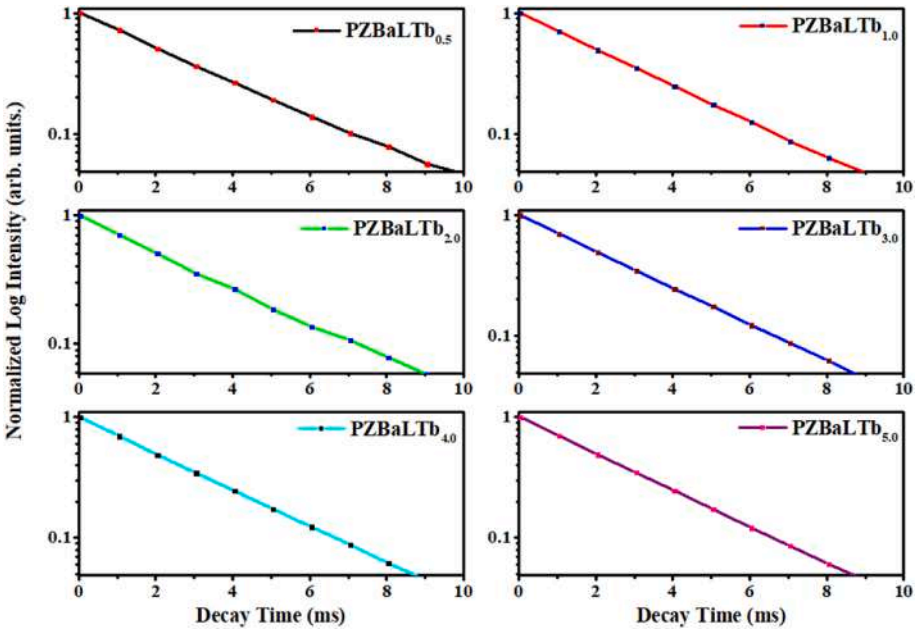


**Fig. 11.** The decay curves of $Tb^{3+}$ doped BZLP glasses at 373 nm excitation and emission at 545 nm.

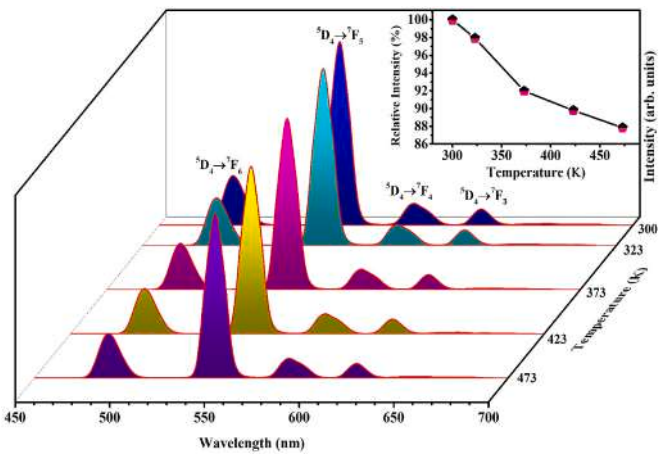


**Fig. 12.** TDPL spectra of $PZBaLTb_{5.0}$ glass with an upsurge in temperature from 300 to 473 K at an excitation wavelength of 373 nm. The inset plot shows the decrease in relative emission intensity with a surge in temperature from 300 to 473 K.

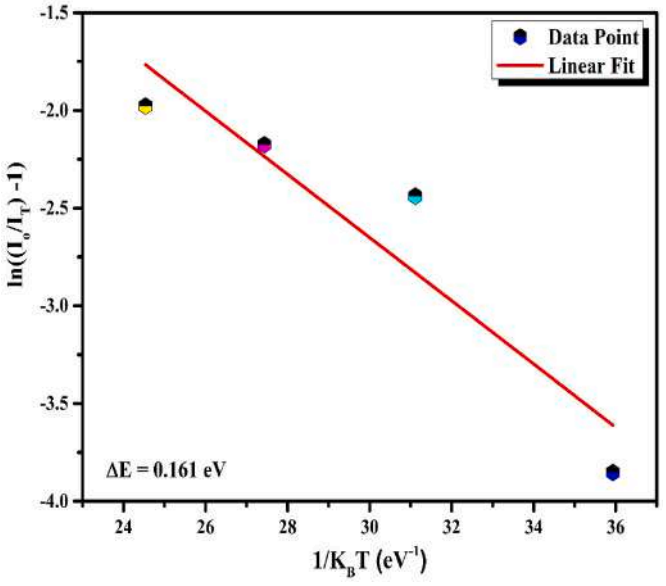


**Fig. 13.** Variation of $\ln[(I_o/I_T)\text{-}1]$ with $(1/K_BT)$ for $PZBaLTb_{5.0}$ glass.

writing the manuscript. **A.S. Rao:** work plan, Supervision, Validation, manuscript correction.

## Declaration of competing interest

The authors declare that they have no known competing financial interests or personal relationships that could have appeared to influence the work reported in this paper.

## Data availability

Data will be made available on request.

## References

[1] A. Jha, B. Richards, G. Jose, T. Teddy-Fernandez, P. Joshi, X. Jiang, J. Lousteau, Rare-earth ion doped $TeO_2$ and $GeO_2$ glasses as laser materials, Prog. Mater. Sci. 57 (2012) 1426–1491, https://doi.org/10.1016/j.pmatsci.2012.04.003.

[2] A.S. Rao, J.L. Rao, S.V.J. Lakshman, Electron paramagnetic resonance and optical absorption spectra of $Cu^{2+}$ ions in alkali cadmium borosulphate glasses, J. Phys. Chem. Solid. 53 (1992) 1221–1226, https://doi.org/10.1016/0022-3697(92)90042-C.

[3] P. Vani, G. Vinitha, M.I. Sayyed, M.M. AlShammari, N. Manikandan, Effect of rare earth dopants on the radiation shielding properties of barium tellurite glasses, Nucl. Eng. Technol. 53 (2021) 4106–4113, https://doi.org/10.1016/j.net.2021.06.009.

[4] A. Kaur, A. Khanna, M. González-Barriuso, F. González, Thermal and light emission properties of rare earth ($Eu^{3+}$, $Dy^{3+}$ and $Er^{3+}$), alkali ($Li^+$, $Na^+$ and $K^+$) and $Al^{3+}$-doped barium tellurite and boro-tellurite glasses, J. Mater. Sci. Mater. Electron. 32 (2021) 17266–17281, https://doi.org/10.1007/s10854-021-06228-3.

[5] N. Deopa, M.K. Sahu, P.R. Rani, R. Punia, A.S. Rao, Realization of warm white light and energy transfer studies of $Dy^{3+}/Eu^{3+}$ co-doped $Li_2O$-PbO-$Al_2O_3$-$B_2O_3$ glasses for lighting applications, J. Lumin. 222 (2020), 117166, https://doi.org/10.1016/j.jlumin.2020.117166.

[6] Y. Zheng, B. Chen, H. Zhong, J. Sun, L. Cheng, X. Li, J. Zhang, Y. Tian, W. Lu, J. Wan, T. Yu, L. Huang, H. Yu, H. Lin, Optical transition, excitation state absorption, and energy transfer study of $Er^{3+}$, $Nd^{3+}$ single-doped, and $Er^{3+}/Nd^{3+}$ co doped tellurite glasses for mid-infrared laser applications, J. Am. Ceram. Soc. 94 (2011) 1766–1772, https://doi.org/10.1111/j.1551-2916.2010.04323.x.

[7] G.C. Righini, F. Enrichi, L. Zur, M. Ferrari, Rare-earth doped glasses and light managing in solar cells, J. Phys. Conf. Ser. 1221 (2019), https://doi.org/10.1088/1742-6596/1221/1/012028.

[8] A. Tamang, A. Hongsingthong, V. Jovanov, P. Sichanugrist, B.A. Khan, R. Dewan, M. Konagai, D. Knipp, Enhanced photon management in silicon thin film solar cells with different front and back interface texture, Sci. Rep. 6 (2016) 1–10, https://doi.org/10.1038/srep29639.

[9] P. Ramprasad, C. Basavapoornima, S.R. Depuru, C.K. Jayasankar, Spectral investigations of $Nd^{3+}$:$Ba(PO_3)_2$+$La_2O_3$ glasses for infrared laser gain media applications, Opt. Mater. 129 (2022), 112482, https://doi.org/10.1016/j.optmat.2022.112482.

[10] A.S. Rao Ravita, Effective energy transfer from $Dy^{3+}$ to $Tb^{3+}$ ions in thermally stable KZABS glasses for intense green emitting device applications, J. Lumin. 239 (2021), 118325, https://doi.org/10.1016/j.jlumin.2021.118325.

[11] A. Kumar, M.K. Sahu Anu, S. Ravita, N. Dahiya, A. Deopa, R. Malik, A.S.Rao Punia, Spectral characteristics of $Tb^{3+}$ doped $ZnF_2$–$K_2O$–$Al_2O_3$–$B_2O_3$ glasses for epoxy free tricolor w-LEDs and visible green laser applications, J. Lumin. 244 (2022), 118676.

[12] A. S.Rao Ravita, Effective sensitization of $Eu^{3+}$ visible red emission by $Sm^{3+}$ in thermally stable potassium zinc alumino borosilicate glasses for photonic device applications, J. Lumin. (2021), 118689, https://doi.org/10.1016/j.jlumin.2021.118689.

[13] J. Gou, J. Fan, S. Zuo, M. Luo, Y. Chen, X. Zhou, Y. Yang, B. Yu, S.F. Liu, Highly thermally stable and emission color tunable borate glass for white-light-emitting diodes with zero organic resin, J. Am. Ceram. Soc. 100 (2017) 4011–4020, https://doi.org/10.1111/jace.14951.

[14] F. Enrichi, C. Armellini, S. Belmokhtar, A. Bouajaj, A. Chiappini, M. Ferrari, A. Quandt, G.C. Righini, A. Vomiero, L. Zur, Visible to NIR downconversion process in $Tb^{3+}$-$Yb^{3+}$ codoped silica-hafnia glass and glass-ceramic sol-gel waveguides for solar cells, J. Lumin. 193 (2018) 44–50, https://doi.org/10.1016/j.jlumin.2017.08.027.

[15] C. Zuo, Z. Zhou, L. Zhu, A. Xiao, Y. Chen, X. Zhang, X. Ding, Q. Ge, Spectroscopic properties of $Ce^{3+}$-doped borosilicate glasses under UV excitation, Mater. Res. Bull. 83 (2016) 155–159, https://doi.org/10.1016/j.materresbull.2016.06.001.

[16] Y. Tayal, A.S. Rao, Orange color emitting $Sm^{3+}$ ions doped borosilicate glasses for optoelectronic device applications, Opt. Mater. 107 (2020), https://doi.org/10.1016/j.optmat.2020.110070.

[17] M. Anand Pandarinath, G. Upender, K. Narasimha Rao, D. Suresh Babu, Thermal, optical and spectroscopic studies of boro-tellurite glass system containing ZnO, J. Non-Cryst. Solids 433 (2016) 60–67, https://doi.org/10.1016/j.jnoncrysol.2015.11.028.

[18] V. Chandrappa, C. Basavapoornima, C.R. Kesavulu, A.M. Babu, S.R. Depuru, C. K. Jayasankar, Spectral studies of $Dy^{3+}$:zincphosphate glasses for white light source emission applications: a comparative study, J. Non-Cryst. Solids 583 (2022), 121466, https://doi.org/10.1016/j.jnoncrysol.2022.121466.

[19] J.F.M. dos Santos, V.S. Zanuto, A.C.C. Soares, E. Savi, L.A.O. Nunes, M.L. Baesso, T. Catunda, Evaluating the link between blue-green luminescence and cross-relaxation processes in $Tb^{3+}$-doped glasses, J. Lumin. 240 (2021), 118430, https://doi.org/10.1016/j.jlumin.2021.118430.

[20] R.T. Karunakaran, K. Marimuthu, S. Surendra Babu, S. Arumugam, Structural, optical and thermal investigations on $Dy^{3+}$ doped NaF–$Li_2O$–$B_2O_3$ glasses, Phys. B Condens. Matter 404 (2009) 3995–4000, https://doi.org/10.1016/J.PHYSB.2009.07.160.

[21] N. Deopa, A.S. Rao, S. Mahamuda, M. Gupta, M. Jayasimhadri, D. Haranath, G. V. Prakash, Spectroscopic studies of $Pr^{3+}$ doped lithium lead alumino borate glasses for visible reddish orange luminescent device applications, J. Alloys Compd. 708 (2017) 911–921, https://doi.org/10.1016/j.jallcom.2017.03.020.

[22] A.S. Rao, Y.N. Ahammed, R.R. Reddy, T.V.R. Rao, Spectroscopic studies of Nd $^{3+}$-doped alkali fluoroborophosphate glasses, Opt. Mater. 10 (1998) 245–252, https://doi.org/10.1016/S0925-3467(97)00055-4.

[23] J.A. Duffy, A common optical basicity scale for oxide and fluoride glasses, J. Non-Cryst. Solids 109 (1989) 35–39.

[24] W.T. Carnall, P.R. Fields, K. Rajnak, Electronic energy levels of the trivalent lanthanide aquo ions. III. Tb $^{3+}$, J. Chem. Phys. 49 (1968) 4447–4449, https://doi.org/10.1063/1.1669895.

[25] K. Jha, M. Jayasimhadri, Spectroscopic investigation on thermally stable $Dy^{3+}$doped zinc phosphate glasses for white light emitting diodes, J. Alloys Compd. 688 (2016) 833–840, https://doi.org/10.1016/j.jallcom.2016.07.024.

[26] H. Tiantian, X.Y. Sun, J. Yu, Y. Gu, L. Xia, Z.X. Wen, H. Guo, X. Ye, Optical properties of $Dy_2O_3$, $Tb_4O_7$ singly doped, $Dy_2O_3/Tb_4O_7$ co doped borogermanate-tellurite glasses for radiation application, J. Lumin. 244 (2022), 118737.

[27] B. Szpikowska-Sroka, N. Pawlik, T. Goryczka, M. Bańczyk, W.A. Pisarski, Influence of activator concentration on green-emitting $Tb^{3+}$-doped materials derived by sol-gel method, J. Lumin. 188 (2017) 400–408, https://doi.org/10.1016/j.jlumin.2017.04.066.

[28] Y.C. Fang, X.R. Huang, Y. der Juang, S.Y. Chu, Color-Tunable blue to green $Ca_4$-$1.5xTa_2O_9$: $xTb^{3+}$ phosphor: cross-relaxation mechanism and thermal stability, J. Am. Ceram. Soc. 95 (2012) 1613–1618, https://doi.org/10.1111/j.1551-2916.2011.05021.

[29] M. Kumar, A.S. Rao, Influence of $Tb^{3+}$ ions concentration and temperature on lithium bismuth alumino borosilicate glasses for green photonic device applications, Opt. Mater. 120 (2021), 111439, https://doi.org/10.1016/J.OPTMAT.2021.111439.

[30] C.K. Jayasankar, K. Upendra Kumar, V. Venkatramu, W. Sievers, T. Tröster, G. Wortmann, Photoluminescence from the $^5D_4$ level of $Tb^{3+}$ ions in K-Ba-Al fluorophosphate glass under pressure, J. Non-Cryst. Solids 353 (2007) 1813–1817, https://doi.org/10.1016/j.jnoncrysol.2007.01.049.

[31] V. Venkatramu, P. Babu, I.R. Martín, V. Lavín, J.E. Muöoz-Santiuste, T. Tröster, W. Sievers, G. Wortmann, C.K. Jayasankar, Role of the local structure and the energy trap centers in the quenching of luminescence of the $Tb^{3+}$ ions in fluoroborate glasses: a high pressure study, J. Chem. Phys. 132 (2010), https://doi.org/10.1063/1.3352631.

[32] C.S. McCamy, Correlated Color Temperature as an Explicit Function of Chromaticity Coordinates, vol. 17, 1992, https://doi.org/10.1002/col.5080170211.

[33] D.H.G. Swati, D. Bidwai, Red emitting $CaTiO_3$: $Pr^{3+}$ nanophosphors for rapid identification of high contrast latent fingerprints, Nanotechnology 31 (2020), 364007.

[34] E.F. Schubert, Light Emitting Diodes, second ed., Cambridge Univ. Press, New York, 2005.

[35] T.M.C.T.W. Kuo, W.R. Liu, High color rendering white light-emitting-diode illuminator using the red-emitting $Eu^{2+}$ activated CaZnOS phosphors excited by blue LED 8187-8192, Opt Express 18 (2010).

[36] C.K.J.K.U. Kumar, P. Babu, Ch Basavapoornima, R. Praveena, D.S. Rani, Spectroscopic properties of $Nd^{3+}$-doped boro-bismuth glasses for laser applications, Phys. B Condens. Matter 646 (2022), 413427.